# Hindered Diffusion of Dextran and Ficoll in Microporous Membranes

**M. P. Bohrer,* Gary D. Patterson, and P. J. Carroll**

*AT&T Bell Laboratories, Murray Hill, New Jersey 07974.* *Received July 29, 1983*

ABSTRACT: The effective diffusivity of a solute within a pore of comparable size is frequently found to be less than its value in bulk solution. This phenomenon is known as "hindered" or "restricted" diffusion and it arises fundamentally from the fact that the characteristic dimension of the solute molecule is no longer small compared to that of the pore through which it passes. Hindered diffusion is observed in a number of important fields such as gel permeation chromatography, heterogeneous catalysis, and membrane separations. Hindered diffusion of narrow molecular weight fractions of two polysaccharides was measured in microporous membranes with well-defined pore geometry. The two polysaccharides examined were dextran, a flexible coiled polymer of 1,6-glucopyranose units, and ficoll, a highly branched copolymer of sucrose and epichlorohydrin. The ratio of the membrane diffusion coefficient ($D$) to the bulk solution diffusion coefficient ($D_\infty$), determined by light scattering, was examined as a function of the relative solute size to membrane pore size ($r_s/r_p$). Values of $D/D_\infty$ were found to be significantly greater for dextran than ficoll over most of the range of $r_s/r_p$ examined. The ficoll data agree very well with a hydrodynamic model of diffusion based on a hard sphere in a tube.

## Introduction

The effective diffusivity of a solute within a pore of comparable size is frequently found to be less than its value in bulk solution. This phenomenon, which is known as "hindered" or "restricted" diffusion, is due to the presence of the pore wall. Hindered diffusion is observed in a number of important fields such as gel permeation chromatography, heterogeneous catalysis, and membrane separations.

Theoretical models of diffusion in fine pores or confined spaces have generally been based either on a hydrodynamic approach or, for the case of long-chain polymers, upon recently developed scaling arguments.[1] Useful discussions of the hydrodynamic treatment of diffusion in porous media are those of Bean,[2] Anderson and Quinn,[3] Brenner and Gaydos,[4] and Malone and Anderson.[5] In general, the porous medium is modeled as an array of identical cylindrical pores. The solute is assumed to have both Brownian and hydrodynamic characteristics and the solvent is treated as a continuum. The latter assumption requires that the solute molecules are sufficiently larger than those of the solvent. In free solution, this treatment leads to Einstein's result

$$D_\infty = kT/f_\infty \tag{1}$$

where $D_\infty$ is the bulk solution diffusion coefficient, $k$ is Boltzmann's constant, $T$ is temperature, and $f_\infty$ is the molecular friction coefficient in bulk solution. For the case of a solid sphere, the familiar Stokes–Einstein equation is obtained where $f_\infty = 6\pi\mu r_s$. The solute radius is given by $r_s$ and $\mu$ is the solvent viscosity.

The apparent diffusion coefficient for a solute in a pore ($D$) is generally found to be less than $D_\infty$. This is due to the combined result of (1) an increase in the hydrodynamic drag above $f_\infty$, due to the pore wall, and (2) steric restriction imposed on the volume available to the solute by the pore wall. Electrostatic or other specific interactions between the solute and pore wall will also contribute to the observed partitioning of solute between the bulk solution and the pore interior. For the case of an uncharged hard sphere, for which the sphere center is sterically excluded from an annular region next to the pore wall equal to its radius, $D/D_\infty$ is given by[3]

$$\frac{D}{D_\infty} = \phi \frac{\int_0^{1-\lambda} [f_\infty/f(\lambda,\beta)]\beta \, d\beta}{\int_0^{1-\lambda} \beta \, d\beta} \tag{2}$$

$$\phi = (1-\lambda)^2$$

where $\lambda = r_s/r_p$, $r_p$ is the pore radius, $\beta$ $(=r/r_p)$ is the dimensionless radial position, and $f(\lambda,\beta)$ is the molecular friction coefficient in the pore. The value of $D/D_\infty$ can be seen to be the product of an equilibrium partitioning coefficient ($\phi$) and an average of $f_\infty/f$ over the accessible cross-sectional area. Unfortunately, values of $f$ are available only for $\lambda \ll 1$.[4] In general, it is assumed that $f(\lambda,0)$ adequately approximates $f(\lambda,\beta)$, leading to

$$\frac{D}{D_\infty} \cong \phi \frac{f_\infty}{f(\lambda,0)} \tag{3}$$

Values of $f(\lambda,0)$ have been obtained numerically by Paine and Scherr[6] among others. The commonly used Renkin[7] equation is identical with eq 3 in which the hydrodynamic results of Faxen (cited in ref 2) have been used to obtain $f_\infty/f(\lambda,0)$.

A second approach to modeling hindered diffusion is based on the scaling theory arguments presented by de Gennes.[1] de Gennes and co-workers have treated both the equilibrium partitioning[8] and the diffusion[9] of polymers in porous media. Cannell and Rondelez[10] have combined these results to examine the effects of $\lambda$ and polymer concentration on $D/D_\infty$. In the dilute concentration regime and for $\lambda > 1$, $D/D_\infty$ is given by

$$D/D_\infty = \alpha\{\beta\lambda^{-2/3} \exp[-(\beta\lambda)^{5/3}]\} \tag{4}$$

where $\alpha$ and $\beta$ are proportionality constants. The scaling theory predicts only the power law behavior for the diffusion and partitioning and does not give precise numerical coefficients.

Quantitative tests of the above theories have been made possible with the development of track-etched membranes of well-defined pore geometry.[11] These membranes, which have generally been made out of mica, polycarbonate, and polyester, contain pores of a uniform radius which can be determined independently of the hindered diffusion measurements. One of the first tests of eq 3 was a study by Beck and Schultz,[12] who measured the diffusion of ribonuclease and several low molecular weight polysaccharides through track-etched mica membranes. They found a good fit of the data for most solutes; however, only a limited range of $\lambda$ values ($<0.2$) was examined. Studies employing polystyrene spheres in track-etched membranes have been performed;[5,14] however, the influence of electrostatic interactions between the spheres and pore wall complicates any comparison with the simple, noninteracting hard-sphere model. Malone and Anderson[5] were

0024-9297/84/2217-1170$01.50/0 

able to reconcile their data with the hydrodynamic theory (eq 3) if electrostatic interactions are included in computing the equilibrium partitioning coefficient. Wong and Quinn[13] measured the diffusion of bovine serum albumin ($\lambda = 0.19$) in mica membranes and found $D/D_\infty$ to be half the predicted value after correcting for protein adsorption. Cannell and Rondelez[10] used polycarbonate membranes to study the diffusion of narrow molecular weight fractions of polystyrene dissolved in ethyl acetate. They also found $D/D_\infty$ to be lower than predicted by eq 3 when the solute radius is calculated from $D_\infty$ using the Stokes–Einstein equation. Their data could be shifted to fit the theoretical curve by increasing the solute radius by 45% for all solutes. Not surprisingly, they also found that eq 4 could be made to fit their data by choosing appropriate values for $\alpha$ and $\beta$. Unfortunately, there is no physical basis to guide the choice of these proportionality constants. It should also be noted that eq 4 is based on the assumption that the polymer chain must be extended in order to enter the pores ($\lambda > 1$), whereas the data reported[10] are for values of $\lambda$ ranging from 0.06 to 0.72.

In a recent study, Deen et al.[15] examined the effect of molecular size and configuration on $D/D_\infty$ by measuring the diffusion of two polysaccharides, dextran and ficoll. Dextran is a slightly branched polymer of D-glucopyranose linked by 1,6 bonds.[16] Branching occurs to the extent of ~5% and most branches contain only one or two monomer units.[17] Ficoll is a cross-linked copolymer of sucrose and epichorohydrin. Due to the different molecular structures of these polymers, they are expected to have different configurations in solution. Measurements of the solution properties of dextran indicate that it behaves as a flexible coiled polymer in aqueous solution.[18] Theoretical studies[19] of molecular conformation of polysaccharides indicate that the $\alpha$-1,6 linkage which connects the D-glucan units in the dextran chain has considerable conformational freedom. The value of the persistence length is predicted to be only 6–13 Å,[19] supporting the view that dextran does not behave as a stiff, extended chain. Ficoll, on the other hand, will be a more compact, rigid type of molecule in solution due to its cross-linked structure. Deen et al.[15] measured the diffusive fluxes of polydisperse samples of dextran and ficoll and then used gel chromatography to obtain the dependence of $D/D_\infty$ on molecular size. The values of $\lambda$ studied were 0.3–0.75 and 0.2–0.45 for dextran and ficoll, respectively. The ficoll data were found to fit eq 3 only for $\lambda = 0.2$–$0.25$ and were lower for larger values of $\lambda$. Dextran was able to diffuse more easily through the membrane since $D/D_\infty$ was found to be significantly higher than either the ficoll data or eq 3. $D/D_\infty$ values for two different dextran experiments were found to show a substantial discrepancy of unknown cause.

In the present study, the findings of Deen et al. have been further investigated by preparing well-defined narrow molecular weight fractions of dextran and ficoll. In this manner, the possible influence of polydispersity and/or changes in the behavior of the gel chromatography column is eliminated. In addition, dynamic light scattering has been used to determine $D_\infty$, independent of the membrane diffusion experiments. Membranes of different pore sizes have been used to determine the effect of $\lambda$ on $D/D_\infty$ and the range of $\lambda$ values examined has been expaned (0.011–1.0 for dextran and 0.007–0.66 for ficoll).

## Experimental Section

Dextran (T70) and ficoll (F70) with molecular weights of ~70 000 were obtained from Pharmacia Fine Chemicals. These samples were fractionated twice on a Sephacryl 300 (Pharmacia) gel column (2.6 cm × 45 cm) using 0.02 M ammonium acetate as eluant. For each fractionation, 23 mL centered at the peak concentration was collected and freeze-dried. For the first fractionation, 0.2 g of the polymer (T70 or F70) in 2 mL of eluant was applied to the top of the gel column and pumped at 1.0 mL/min. The second fractionation was identical with the first except that only 0.1 g of the polymer in 2 mL of eluant was added. Weight-average molecular weights ($M_w$) were measured by light scattering (KMX-6 low-angle light scattering photometer, Chromatix) and number-average molecular weights ($M_n$) were measured by membrane osmometry (Wescan Instruments). Values of the refractive index increment ($dn/dc$) were also measured for each fraction (laser differential refractometer, Chromatix).

The average self-diffusion coefficient $\bar{D}_\infty$ was determined by photon correlation spectroscopy. The incident light was at 5145 Å and the scattering was observed at 90°. The single-clipped photocount autocorrelation function was obtained with a Malvern correlator. The average mutual diffusion coefficient was obtained at each concentration by the method of cumulants. The results were extrapolated to infinite dilution to obtain $D_\infty$. Full details of the experimental procedures are published elsewhere.[20,21]

Track-etched polycarbonate membranes with nominal pore radii of 25, 75, 250, 500, and 5000 Å were obtained from Nuclepore Corp. These membranes contain pores that are essentially uniform circular cylinders.[22] The membrane thickness was obtained from the weight/area of the membrane using the density of polycarbonate and a slight correction to account for the small number of pores which are not aligned exactly perpendicular to the membrane surface.[23] Scanning electron microscope (SEM) photographs (500–15 000× magnification) were used to obtain pore densities, and pore radii were determined from water flow measurements as described previously.[23]

Diffusion experiments were done by using a stirred diffusion cell constructed from Lucite similar to that described elsewhere.[15] The membrane is held between two annular discs which are clamped between two identical cell chambers. The volume of each chamber is 39.1 $cm^3$ and the exposed membrane area is 11.4 $cm^2$. Teflon-coated magnetic stirring disks epoxied to stainless steel shafts were rotated at 100 rpm (±1 rpm) by an external magnet connected to a motor with an optical tachometer. The diffusion cell is jacketed for temperature control (25.0 ± 0.1 °C) and each cell contains an inlet and outlet port for sampling. The difference in concentration between each chamber was recorded continuously by pumping the solution from each chamber through separate cells of a differential refractive index monitor (Waters Associates) and then back to the diffusion cell. Differences in concentrations as low as 0.001 g/100 mL could be detected. To ensure that the concentration measured was representative of the concentration in the cell chamber, the fluid was pumped at a sufficiently high rate relative to the transmembrane diffusion rate. For experiments lasting longer than ~6 h, samples were taken periodically for analysis rather than continuously. Conservation of mass for the diffusion cell indicates that the concentration difference ($\Delta C$) between the two chambers is given by

$$\ln\left[\frac{\Delta C_0}{\Delta C}\right] = \frac{2At}{VR} \tag{5}$$

where $\Delta C_0$ is the concentration difference at time ($t$) = 0, $A$ is the exposed membrane area, $V$ is the cell volume, and $R$ is the total mass transfer resistance. $D$ is related to $R$ by

$$R = \frac{L}{n\pi r_p^2 D} + R_b \tag{6}$$

where $L$ is the membrane thickness, $n$ is the pore density, and $R_b$ represents the boundary layer resistance to mass transport on both sides of the membrane as well as a correction for the fact that diffusion is not one-dimensional near the membrane.[23]

The procedure used for the diffusion experiments was similar in each case. Initially, one chamber was filled with an aqueous solution of the solute (0.02–0.05 g/100 mL) while the other side was filled with deionized water. The slope of a plot of $\ln(\Delta C_0/\Delta C)$ vs. $t$ was obtained by linear regression, and regression coefficients usually exceeded 0.99. The time of the diffusion experiments varied from about 30 min for the largest pore membrane to ~9 days for the smallest pore size.

**Table I**
**Properties of Dextran and Ficoll Fractions**

| polymer | $M_w$ | $M_n$ | $M_w/M_n$ | $D_\infty$, cm$^2$/s | $r_s$[a] Å |
|---|---|---|---|---|---|
| dextran | 51 000 | 43 700 | 1.17 | $4.0 \times 10^{-7}$ | 61 |
| ficoll | 48 200 | 44 800 | 1.08 | $6.2 \times 10^{-7}$ | 40 |

[a] Stokes–Einstein radius, calculated with $D_\infty$ given in column 5.

As discussed in a separate publication,[23] the diffusional boundary layer resistance ($R_b$) can often be a significant fraction of $R$ and must therefore be accounted for in order to properly interpret the experimental results. The procedure described previously[23] was used in the present study to determine $R_b$. Briefly, this involves measuring the diffusion of a small solute (glucose or sucrose) for which the diffusivity is known. Use of eq 5 in which $D_\infty$ is substituted for $D$ allows calculation of $R_b$ for that particular membrane and stirring speed.

## Results

The dextran and ficoll characterization results are shown in Table I. The polydispersity of the fractions as represented by the ratio $M_w/M_n$ was found to be 1.17 and 1.08 for dextran and ficoll, respectively. This compares to 1.26 for dextran (T70) and 1.63 for ficoll (F70) for the original samples as reported by Pharmacia. Values of $dn/dc$ were found to be 0.148 (dextran) and 0.149 (ficoll). The values of $D_\infty$ obtained from the light scattering experiments are shown in column 5 and the values of $r_s$ (Stokes–Einstein radius) are given in column 6.

The membrane parameters determined from the membrane weights, water flow measurements, and SEM photographs are shown in Table II. The measured values of $L$, $r_p$, and $n$ are estimated to be accurate to ±1%, ±2%, and ±5%, respectively. The measured values of $r_p$ are significantly higher than the nominal sizes reported by the manufacturer. Also included in Table II are the values of $R_b$ determined for each membrane based on the diffusion of glucose and sucrose. Values are given for both dextran and ficoll since $R_b$ depends upon $D_\infty$. It is interesting to note that $R_b$ increases for the lowest porosity ($n\pi r_p^2$) membranes, a finding in agreement with that reported previously.[23]

The adsorption of dextran or ficoll on the polycarbonate membranes, an effect which would alter the pore dimensions and interfere with the diffusion experiments, was examined previously.[15] No adsorption was detected for either polymer.

The hindered diffusion data for dextran and ficoll are given in Table III and presented graphically in Figure 1 (data points). The solid curve is eq 3 using the hydrodynamic results of Paine and Scherr.[6] The ficoll data can be seen to follow eq 3 rather closely, whereas the dextran data are significantly greater over the entire range of $r_s/r_p$ values except possibly at $r_s/r_p \to 0$.

## Discussion

The close fit of the ficoll hindered diffusion data (Figure 1) to eq 3 indicates that the model of a hard sphere in a tube is a good approximation for this particular polysaccharide. This is not surprising in view of the highly branched or "cross-linked" nature of this polymer, which would tend to give it a rigid, globular-type conformation. Dextran, which is best modeled as a flexible coiled polymer,[18,19] diffuses more readily through the pores than ficoll with an equivalent bulk solution diffusion coefficient. Apparently, the flexibility of the dextran molecule allows it to accommodate itself more easily within the confined spaces of the pores. In fact, even when the dextran Stokes–Einstein radius equals the pore radius, there is a measurable diffusion rate as evidenced by the value of $D/D_\infty = 0.038$ at $r_s/r_p = 1.0$. According to the hard-sphere model, there should be no diffusion at $r_s/r_p = 1.0$ since the partitioning ($\phi = (1 - r_s/r_p)^2$) drops to 0. For $r_s/r_p \to 0$, i.e., very little hindrance, the value of $D/D_\infty$ for both dextran and ficoll can be seen to approach a value of 1, indicating good agreement between the light scattering and membrane diffusion method for determining $D_\infty$.

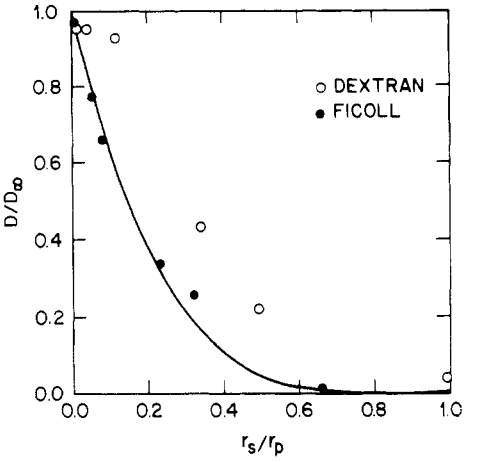


**Figure 1.** Ratio of the pore-to-bulk diffusivities for dextran and ficoll as a function of the ratio of Stokes–Einstein radius to pore radius. The solid curve is calculated from eq 3 using $f(\lambda,0)$ from Paine and Scherr.[6]

It should be noted that since the dextran and ficoll samples are not perfectly monodisperse (see Table I), the diffusion results may be influenced to some extent by this polydispersity. In particular, if the dextran contains a greater fraction of low molecular weight components than does ficoll, it would be expected to have a higher diffusivity for short-time measurements. For all but the smallest pore size, the experimental time period was sufficient to allow at least 12% of the polymer to diffuse through the membrane. In addition, the diffusion cell was run for 1–3 days prior to making any measurements to permit any very small solutes to equilibrate. The fact that successive measurements of the diffusion coefficient for a given experiment were found to vary about the mean, and not steadily decrease, is an indication that the polydispersity was not sufficient to significantly affect the measured diffusion coefficients. This was found to be true for both dextran and ficoll.

**Table II**
**Membrane Characterization**

| membrane no. | $L$, μm | $r_p$, Å | $n$, cm$^{-1}$ | $n\pi r_p^2$ | $R_b$, s/cm dextran | $R_b$, s/cm ficoll |
|---|---|---|---|---|---|---|
| 1.0 N/B | 11.1 | 5810 | $1.88 \times 10^7$ | 0.199 | 20 400 | 15 200 |
| 0.1 N/A | 6.68 | 747 | $3.56 \times 10^8$ | 0.062 | 18 000 | 13 400 |
| 0.05 N/A | 6.40 | 498 | $6.55 \times 10^8$ | 0.051 | 17 400 | 13 000 |
| 0.015 N2/A | 6.53 | 177 | $6.15 \times 10^8$ | 0.006 | 29 600 | 22 100 |
| 0.015 C2/C | 6.59 | 124 | $7.49 \times 10^8$ | 0.004 | 403 000 | 301 000 |
| 0.005 C/B | 6.84 | 61 | $3.46 \times 10^9$ | 0.004 | 667 000 | 498 000 |

**Table III**
**Hindered Diffusion Data**

| dextran | | ficoll | |
|---|---|---|---|
| $r_s/r_p$ | $D/D_\infty$ | $r_s/r_p$ | $D/D_\infty$ |
| 0.011 | 0.95 | 0.007 | 0.97 |
| 0.082 | 0.95 | 0.054 | 0.77 |
| 0.12 | 0.93 | 0.080 | 0.66 |
| 0.34 | 0.43 | 0.23 | 0.34 |
| 0.49 | 0.22 | 0.32 | 0.26 |
| 1.00 | 0.038 | 0.66 | 0.018 |

In a previous study[15] using the same macromolecules, qualitatively similar results were found in that the values of $D/D_\infty$ were greater for dextran than ficoll of equivalent size (Stokes–Einstein). In the previous study, however, the values of $D/D_\infty$ for ficoll were found to be lower than predicted by the hydrodynamic model for most of the range of $r_s/r_p$ examined ($0.25 \leq r_s/r_p \leq 0.45$). As mentioned above, this discrepancy may be due to uncertainty or changes in the gel chromatography column used in the previous study. In that study, it was necessary to fractionate samples from two separate diffusion experiments, one using a large pore membrane to get $D_\infty$ and one using a small pore membrane to get $D$. These fractions then had to be matched exactly in order to get the ratio $D/D_\infty$. Any changes in the behavior of the gel column would therefore cause a change in the calculated values of $D/D_\infty$. This may also explain why two different sets of results were obtained for dextran in that study. The dextran data in the present study compare favorably with one of these sets of results. In particular, the values of $D/D_\infty$ for $r_s/r_p = 0.34$ and 0.49 are 0.43 and 0.22 (Figure 1), which compares to ~0.45 and 0.21 taken from the lower curve in ref 15.

An additional factor that may be responsible for at least part of the discrepancy noted between the present results for ficoll and those reported previously[15] could be the determination of the diffusional boundary layer resistance. In the study by Deen et al.,[15] $R_b$ was determined by measuring the diffusion of several small solutes in a membrane with a porosity of 4.8%. This value of $R_b$ was then used in the calculation of the hindered diffusion results which were obtained with membranes with porosities of 0.18%. A recent study by Bohrer,[23] however, indicates that $R_b$ increases as the porosity of the membrane decreases below ~6%. Although data are not available for membrane porosities as low as 0.18%, the results of the present study show that $R_b$ increases dramatically (~35-fold, Table II) with decreasing porosity. Thus, even though $R_b$ represents only a small fraction of $R$ (<1% reported in ref 15), it is possible that $R_b$ was grossly underestimated. Increasing $R_b$ would cause the values of $D/D_\infty$ calculated in ref 15 to be increased for both dextran and ficoll.

As noted above, a number of studies have examined the effect of molecular size on hindered diffusion. There have been relatively few studies, however, of the influence of molecular configuration and/or flexibility on hindered diffusion. In a previous study using dextran and ficoll, Bohrer et al.[24] compared ultrafiltration rates of these macromolecules across the walls of glomerular capillaries of rat kidneys in vivo. Normalized filtration rates of dextran were found to exceed those of ficoll at any given molecular size as determined by gel chromatography. These results are in qualitative agreement with the present study; however, uncertainty in the pore structure of the capillary walls precludes any comparison with the theoretical model.

Colton et al.[25] measured the diffusion and partitioning of polystyrene and two proteins in porous glass cubes reported to have narrow pore size distributions. They observed that the equilibrium partitioning of the polystyrene and proteins behaved similarly, decreasing as $\lambda(r_s/r_p)$ increased. Diffusional results indicated that the friction coefficient for the polystyrene was unchanged within the pores ($f = f_\infty$) whereas the proteins followed the hard-sphere prediction. These results were interpreted as indicating a free-draining type of behavior for the polystyrene where the relevant frictional length scale is closer to that of a monomer unit rather than the overall molecular dimensions.

Finally, Schultz et al.[26] measured osmotic water flow through well-characterized track-etched membranes for a variety of proteins and dextran. For the same molecular size, proteins were found to have larger reflection coefficients than dextrans, indicating less resistance to transport for the dextrans. They attribute this difference to the greater flexibility of dextran, which allows it to assume a smaller molecular size within the membrane.

The results of the present study and those cited above clearly indicate that molecular configuration or the ability to change configuration is an important determinant of the diffusive movement of solutes within confined spaces. The use of well-defined pore geometry in this study permits a direct comparison with the hydrodynamic model of a hard sphere in a tube. Excellent agreement between this model and the ficoll data was observed. Dextran was found to diffuse more readily through the membrane than ficoll of an equivalent Stokes–Einstein radius, presumably due to its greater ability to deform within the membrane pores.

**Acknowledgment.** We gratefully acknowledge the assistance of Mr. L. Stillwagen in measuring the polymer molecular weights.

## References and Notes

(1) de Gennes, P. G. "Scaling Concepts in Polymer Physics"; Cornell University Press: Ithaca, NY, 1979.
(2) Bean, C. P. In "Membranes"; Eisenman, G., Ed.; Marcel Dekker: New York, 1972; Vol. 1, p 1.
(3) Anderson, J. L.; Quinn, J. A. *Biophys. J.* **1974**, *14*, 130.
(4) Brenner, H.; Gaydos, L. J. *J. Colloid Interface Sci.* **1977**, *58*, 312.
(5) Malone, D. M.; Anderson, J. L. *Chem. Eng. Sci.* **1978**, *33*, 1429.
(6) Paine, P. L.; Scherr, P. *Biophys. J.* **1975**, *15*, 1087.
(7) Renkin, E. M. *J. Gen. Physiol.* **1954**, *38*, 225.
(8) Daoud, M.; de Gennes, P.-G. *J. Phys. (Paris)* **1977**, *38*, 85.
(9) Brochard, F.; de Gennes, P.-G. *J. Chem. Phys.* **1977**, *67*, 52.
(10) Cannell, D. S.; Rondelez, F. *Macromolecules* **1980**, *13*, 1599.
(11) Price, P. B.; Walker, R. M. *J. Appl. Phys.* **1962**, *33*, 3407.
(12) Beck, R. E.; Schultz, J. S. *Biochim. Biophys. Acta* **1972**, *255*, 273.
(13) Wong, H. J.; Quinn, J. A. In "Colloid and Interface Science"; Kerker, M., Ed.; Academic Press: New York, 1976; Vol. 5, p 169.
(14) Conlon, T.; Craven, B. *Aust. J. Chem.* **1972**, *25*, 695.
(15) Deen, W. M.; Bohrer, M. P.; Epstein, N. B. *AIChEJ* **1981**, *27*, 952.
(16) Granath, K. A. *J. Colloid Sci.* **1958**, *13*, 308.
(17) Larm, O.; Lindberg, B.; Svensson, S. *Carbohydr. Res.* **1971**, *20*, 39.
(18) Basedow, A. M.; Ebert, K. H. *J. Polym. Sci., Polym. Symp* **1979**, *No. 66*, 101.
(19) Brant, D. A.; Burton, B. A. In "Solution Properties of Polysaccharides"; Brant, D. A., Ed., American Chemical Society: Washington, DC, 1981; p 81.
(20) Patterson, G. D.; Stevens, J. R.; Alms, G. R.; Lindsey, C. D. *Macromolecules* **1979**, *12*, 658.
(21) Patterson, G. D.; Jarry, J.-P.; Lindsey, C. P. *Macromolecules* **1980**, *13*, 668.
(22) Liabastre, A. A.; Orr, C. *J. Colloid Interface Sci.* **1978**, *64*, 1.
(23) Bohrer, M. P. *Ind. Eng. Chem. Fundam.* **1983**, *22*, 72.
(24) Bohrer, M. P.; Deen, W. M.; Robertson, C. R.; Troy, J. L.; Brenner, B. M. *J. Gen. Physiol.* **1979**, *74*, 583.
(25) Colton, C. K.; Satterfield, C. N.; Lai, C.-J. *AIChEJ* **1975**, *21*, 289.
(26) Schultz, J. S.; Valentine, R.; Choi C. Y. *J. Gen. Physiol.* **1979**, *73*, 49.